ORIGINAL PAPER

Silver particles-modified polysulfonic acid-doped polyaniline layers: electroless deposition of silver in slightly acidic and neutral solutions

Vladimir Lyutov · Vessela Tsakova

Abstract Polyaniline layers are produced by electrochemical polymerisation of aniline in the presence of small amounts of poly(2-acryalamido-2-methyl-propane-sulfonic acid) in an inorganic acid solution. Electroactivity and in situ conductance of the obtained polysulfonic acid-doped layers are studied in slightly acidic and neutral solutions. Electroless deposition of silver particles is carried out in silver-EDTA complex ion solutions at pH=4.2 and pH=6.6 by using the polyaniline layers as reductant. The amount of electroless-deposited silver is studied depending on: polymerisation charge used to synthesize the polymer layer, pH of the plating solution, metal ion concentration and dipping time. SEM shows in all cases a highly non-homogeneous distribution of the metallic phase over the surface, the most protruding fibrillar polymer structures favouring the electroless silver deposition. A linear dependence between amount of the polyaniline material and amount of deposited silver is found for the silver plating solutions with the highest investigated concentration (10 mmol l^{-1}). At lower concentrations (2.0 and 0.4 mmol l^{-1}), the same amount of silver becomes deposited on polymer layers with markedly different charges. The electroless deposition of silver in the solutions with lower acidity results in lower amounts of deposited silver at otherwise identical conditions. Effects such as charge transfer within the polymer phase and mass transport in the solution are addressed to explain the observed dependencies of the amount of deposited silver on concentration and pH in the different plating solutions.

V. Lyutov · V. Tsakova (✉)
Institute of Physical Chemistry,
Bulgarian Academy of Sciences, 1113,
Sofia, Bulgaria
e-mail: tsakova@ipc.bas.bg

Introduction

Polyaniline (PANI) is one of the well-known and intensively studied conducting polymer materials [1]. Different approaches are used to produce PANI-based composites containing various metals [2, 3]. In recent years, the synthesis of Ag-containing PANI composites has attracted considerable interest [4–27]. The prevailing part of the studies address chemical synthesis approaches relying either on one-pot synthesis (combining polymerisation of the monomer and reduction of metal ions) [4–16] or oxidative–reductive reaction occurring in solution between dissolved polymer species and metal ions [17–21]. Few studies [22–24] are directed to the possibility to use supported PANI layers with electrochemically controlled initial oxidation state for electroless silver particles deposition by using the reduced polymer as reductant for metal ions. An alternative to the chemical methods for producing Ag-PANI composites provides the electrodeposition of silver on supported polymer layers [23, 25–27]. This approach has resulted so far in the formation of small amounts of metal particles on the PANI surface [23, 25–27]. In contrast to both the oxidative–reductive approach for producing metal-polymer composites in solutions and the electrodeposition approach, the electroless metal deposition on supported conducting polymer layers provides suitable opportunities for tuning the metal deposition process including also increase of the number of deposited particles [23, 28].

In the last years, silver-modified electrodes are intensively studied in view of various applications, e.g. for electrochemical detection of hydrogen peroxide [29–31],

glucose [32], cytochrome c [33], dopamine and ascorbic acid [34], hydrazine [35], halides [36], cyanides [37] etc. as well as a component for antibacterial coatings [38]. Bearing in mind this broad scope of applications, it is important to be able to influence in an easy and effective way the amount and surface coverage of the metallic phase deposited on supported conducting polymer layers.

Recently, we have investigated the polymerisation of aniline in the presence of small amounts of a polysulfonic acid, poly(2-acryalamido-2-methyl-propane-sulfonic acid) (PAMPSA) in inorganic acid solutions [39, 40]. It was established that PAMPSA becomes immobilised in the PANI structure. Moreover, PAMPSA-doped PANI layers preserve their electroactivity in neutral and slightly alkaline solutions (with acidities of up to pH=9). The aim of the present investigation is to study the electroless deposition of silver in PAMPSA-doped PANI layers at two different pH values (4.2 and 6.6) of the metal plating solution and to obtain Ag-PANI composite materials with preserved electroactivity in neutral solutions. Before addressing this goal, it was first necessary to investigate the pH behaviour of the PANI/PAMPSA layers in slightly acidic solutions and to get some insight into the surface morphology and in situ conductivity of PAMPSA-doped PANI in this pH range.

Experimental

All experiments were carried out in three electrode arrangement at room temperature. A platinum plate was used as counter electrode and mercury/mercury sulphate (Hg/Hg$_2$SO$_4$/sat. K$_2$SO$_4$) (MSE) served as reference electrode. Three different types of working electrodes were used: (1) single crystal polyfaced platinum bead ($S=5.6 \times 10^{-3}$ cm^2), melted in a glass tube, for the electrochemical measurements; (2) platinum plates ($S=2$ cm^2) for the preparation of specimens for SEM imaging; and (3) interdigitated gold electrodes ($S=2.5 \times 10^{-3}$ cm^2) for the in situ conductance measurements [41–43]. The experiments were performed by means of a computerised potentiostat/galvanostat (AUTOLAB PGSTAT 30, Ecochemie). Before measurements, the electrolyte solutions were de-aerated by bubbling with argon for at least 15 min. All potentials in the text and figures are given with respect to MSE.

The electropolymerisation of PAMPSA-doped PANI layers was carried out in aqueous solution of 0.055 mol l^{-1} aniline, 0.4 mol l^{-1} HClO$_4$ and 7 mmol l^{-1} (per monomer unit) PAMPSA (Aldrich, 15 wt.% in water, Mw of ~2,000,000) at constant potential $E=0.32$ V. The polymerisation charge, q_{poly} was used as a measure for the amount of electrodeposited polyaniline. By means of microgravimetric measurements [40] and assuming that the density of the PAMPSA-doped PANI is 1 g l^{-1}, it can

roughly be estimated that at $q_{poly}=14$ mC cm^{-2}, the thickness of the polymer layer is about 200 nm. After synthesis, the PANI-coated electrodes were transferred into supporting electrolyte (0.4 mol l^{-1} HClO$_4$) and subjected to several oxidation/reduction cycles. The reduction charge, q_{red} of the layer was determined in a potentiodynamic sweep between −0.66 and 0.32 V. PAMPSA-doped PANI layers with various polymerisation charges were produced by extending the duration of the electropolymerisation. The relationship between polymerisation and reduction charges for PAMPSA-doped PANI layers produced in mixed PAMPSA-perchloric acid solutions is linear in the entire studied range of polymerisation charges (Fig. 1). The slope $dq_{red}/dq_{poly}=0.20$ is about two times higher than the corresponding slope obtained for PANI layers electrosynthesized in mixed PAMPSA-sulfuric acid solutions [39].

Investigations of the pH dependence of the electrochemical activity and conductance of the PAMPSA-doped PANI layers were carried out in buffer solutions with the following compositions: (1) 0.1 mol l^{-1} NaCl+ 10 mmol l^{-1} CH$_3$COOH/CH$_3$COONa for the pH range from 4 to 5 and (2) 0.1 mol l^{-1} NaCl+10 mmol l^{-1} Na$_2$HPO$_4$/NaH$_2$PO$_4$ for the pH range from 6 to 7.

In situ four-point conductance measurements were carried out by applying potential pulses of 50 mV with alternating polarity between the outer strips of specially designed interdigitated electrodes consisting of four comb-like structured gold strips. The current is measured through the outer and the voltage between the inner strips. A detailed description of the measurement technique and the electrodes can be found in Refs. [41–43].

Silver-EDTA plating solutions with different concentrations (10.0, 2.0 and 0.4 mmol l^{-1}) of Ag were prepared by mixing aqueous solution of AgNO$_3$ with the corresponding concentration of silver ions with aqueous solution of
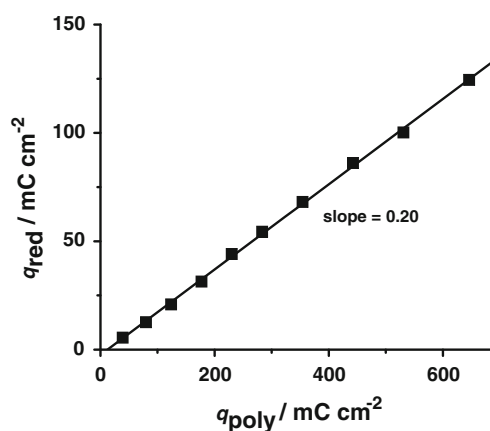
Fig. 1 Dependence of the reduction charge q_{red} on the polymerisation charge q_{poly} for PAMPSA-doped PANI layers synthesized in mixed HClO$_4$/PAMPSA acid solutions

0.02 mol l^{-1} Na$_2$C$_{10}$H$_{14}$O$_8$N$_2$ (disodium salt of ethyl-enediaminetetraacetic acid) and 0.5 mol l^{-1} KNO$_3$. Thus solutions with pH=4.2 were obtained. Ag-EDTA plating solutions with pH=6.6 were adjusted by addition of KOH. EDTA is a hexadentate ligand that forms stable chelates with most metal cations in a 1:1 ratio In the case of silver, the formation of the [AgEDTA]$^{3-}$ complex with stability constant $\beta=2.1\times10^7$ is described in the literature [44]. This trivalent complex should predominate in neutral and alkaline solutions. Based on the data for the composition of the EDTA solutions as a function of pH [44], the formation of the divalent [AgHEDTA]$^{2-}$ complex should be expected in slightly acidic solutions (e.g. pH=4.2). The equilibrium potentials of silver in the 2 mM Ag-EDTA plating solutions were measured to be $E_{Ag}^0=-0.021$ V for pH=4.2 and $E_{Ag}^0=-0.114$ V for pH=6.6.

Before dipping the PANI-coated electrodes in the silver plating solution the PANI layers were subjected to reduction by keeping the electrodes in supporting electrolyte (0.4 mol l^{-1} HClO$_4$) at -0.62 V for at least 15 min. After disconnecting the electrodes, they were immediately dipped in the silver plating solution, typically for 15 s. In a next step the amount of deposited silver was measured in the supporting electrolyte by means of a slow oxidative scan (at 5 mV s^{-1}) starting from $E=-0.3$ V in the positive direction up to $E=0.32$ V. Complete oxidation of the available silver species was observed in this voltammetric scan as evidenced by electrochemical measurements (subsequent scans in the same potential window) and SEM. By integration of the silver dissolution peak currents, the charge q_{Ag} corresponding to the electroless-deposited silver was obtained.

Imaging of the surface structure of PAMPSA-doped PANI layers and of the silver deposit was performed by means of a JSM 6390 (Jeol) scanning electron microscope.

Results and discussion

Oxidation–reduction behaviour of PAMPSA-doped PANI in slightly acidic solutions

The voltammetric behaviour of a PAMPSA-doped PANI layer in solutions with different acidities in the range pH=0.4 to pH=7 is shown in Fig. 2. The measurement is carried out with a relatively thin ($q_{poly}=38$ mC cm^{-2}) PANI layer. The typical, two redox peak structure of the voltammetric curve (corresponding to transitions from leucoemeraldine to emeraldine at more negative potentials and from emeraldine to pernigraniline at more positive potentials) is registered in acidic solution. With increasing pH both peaks gradually merge and transform finally (at pH=7) into a single redox peak. This behaviour is reversible and the double peak
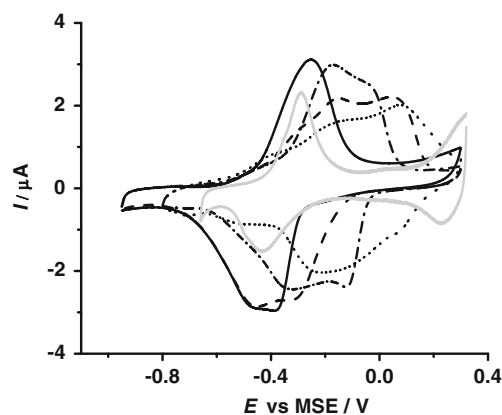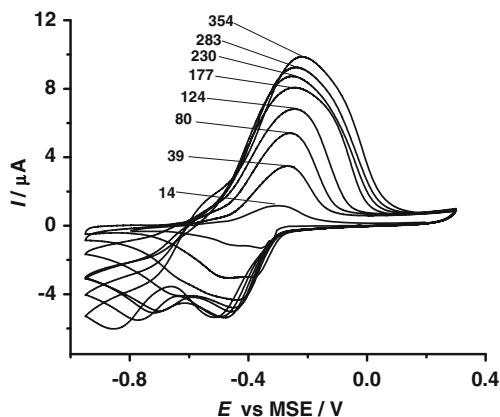

Fig. 2 Cyclic voltammograms measured in solutions with different acidities at a PAMPSA-doped PANI layer ($q_{poly}=39$ mC cm^{-2}): pH= 0.4 (grey line), pH=4.0 (black, dotted line), pH=5.0 (black, dashed-dotted line), pH=6.0 (black, dashed line) and pH=7.0 (black, full line). Scan rate, 20 mV s^{-1}

voltammogram is recuperated by transferring the electrode back into acidic solution (Fig. 1, grey line). A similar pH behaviour of the voltammetric response was already observed for self-doped and other polyacid-doped PANIs [45–48] and explained by taking into account different pH dependencies of both redox processes. In our recent study [40] on PAMPSA-doped PANI, we discussed the mechanism of the redox reactions occurring in neutral solution. It was suggested that due to the formation of a stable PANI–PAMPSA complex, the emeraldine salt state of PANI becomes stabilized in neutral and slightly alkaline solutions (up to pH=9) and the oxidative process involves a transition from leucoemeraldine base to emeraldine salt and from emeraldine salt to pernigraniline base, both reactions occurring in a very narrow potential window. In the pH range relevant for this study (pH=4.2 and pH=6.6), the PAMPSA-doped PANI layers preserve high electroactivity.

A further insight into the behaviour of PAMPSA-doped PANI in neutral solutions was obtained by studying the voltammetric behaviour at different polymerisation charges of the polymer layers (Fig. 3). With increasing thickness, the reductive peak centered at about -0.5 V reaches a saturation value and a second reduction peak emerges at more negative potentials showing a strongly inhibited reductive process that remains uncompleted at the negative potential limit used in these experiments. There are different reasons that might explain the appearance of the second reduction peak in Fig. 3, e.g. change in the morphology and/or in the conductivity with increasing thickness of the polymer layers.

In order to address these possibilities PAMPSA-doped PANI layers obtained through different polymerisation charges were inspected by SEM (Fig. 4). It is clearly seen that with increasing polymerisation charge, the surface

Fig. 3 Cyclic voltammograms measured in buffer solution, pH=7.0, at PAMPSA-doped PANI layers with different polimerisation charges marked by figures in mC cm^{-2}. Scan rate, 20 mV s^{-1}

structure of the PANI layers evolves from a compact globular layer (Fig. 4a, b) to a less dense and looser fibrillar upper structure (Fig. 4c, d). Fig. 4d shows clearly the existence of both structures in a defect of a thick polymer layer. The transition from the bottom, dense layer to the upper fibrillar structure starts at q_{poly} close to 27 mC cm^{-2}. At q_{poly}=80 mC cm^{-2}, the building of a

closed fibrillar upper layer is not yet completed. At polymerisation charges exceeding this value, the fibrillar structure gradually builds a complete upper layer. Despite of the structural changes of the PAMPSA-doped PANI layers with thickness, there is no influence of the morphology on the ratio between polymerisation and reduction charge, measured in acidic solution (Fig. 1). On the other hand the change in morphology with thickness correlates with the emergence of the second, more negative reduction peak, observed in neutral solutions. In this media, however, the conductivity of the PANI layer is expected to be significantly diminished.

Figure 5 shows in situ conductance measurements at a PAMPSA-doped PANI layer as a function of potential at four different pH values. The potential region of high conductivity shifts with pH in consistence with the pH dependence of the voltammetric curves. There is a significant difference (by about two order of magnitudes) in the maximal conductance at the two pH values (pH=4.2 and pH=6.6) used further for electroless silver plating. Polymer layers with large polymerisation charges (q_{poly}= 120 mC cm^{-2}) are used in these experiments because of the necessity to bridge the gaps between the conducting strips of the comb-like structured gold electrodes. Thus, the in
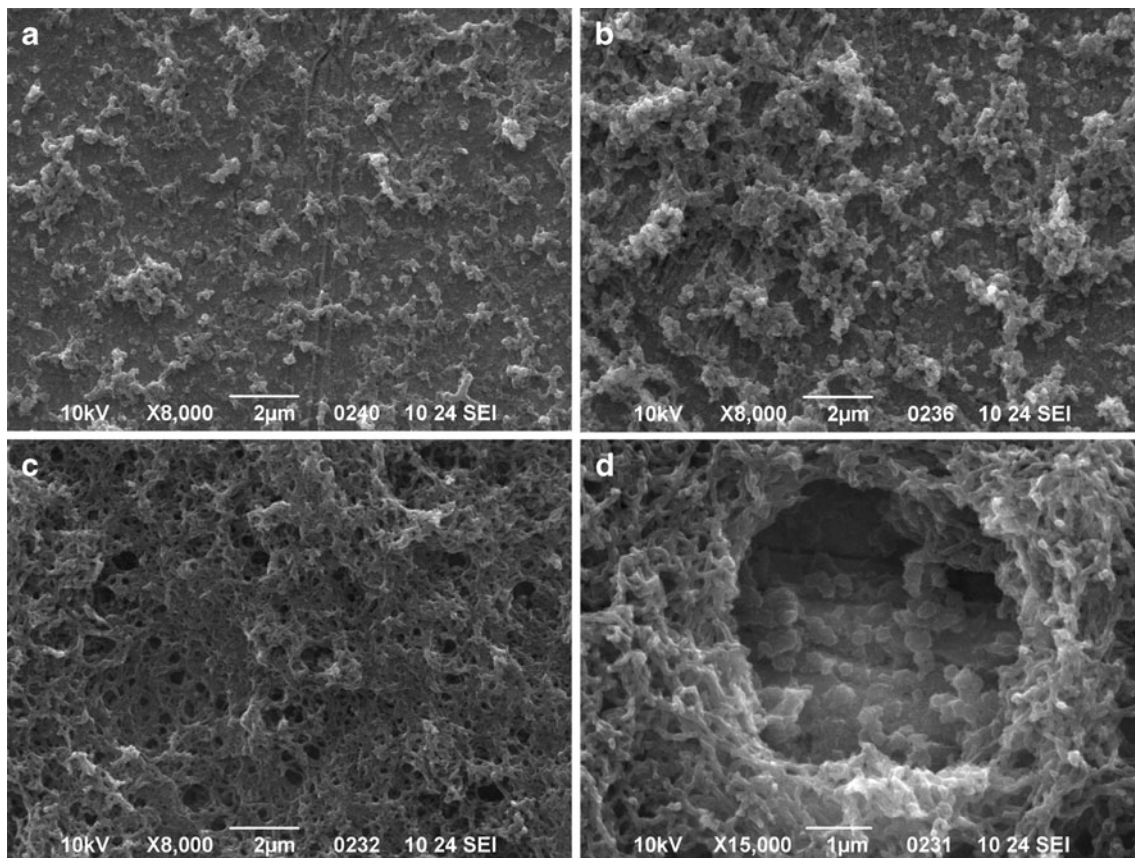
**Fig. 4** SEM of PAMPSA-doped PANI layers with q_{poly}: **a** 27 mC cm^{-2}, **b** 80 mC cm^{-2} and **c, d** 353 mC cm^{-2}
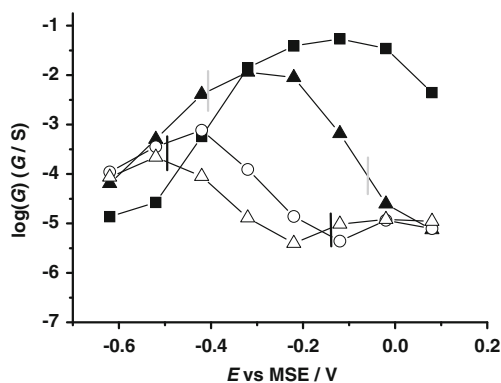
Fig. 5 In situ conductance measurements at a PAMPSA-doped PANI layer (q_{poly}=120 mC cm^{-2}) in solutions with different acidities: pH=2 (*closed squares*), pH=4 (*closed triangles*), pH=6 (*open circles*) and pH=7 (*open triangles*). *Straight lines* denote the potential intervals where OCP varies in the course of silver electroless deposition at pH= 4.2 (*grey lines*) and pH=6.6 (*black lines*)

situ conductance measurements correspond to PAMPSA-doped PANI layers with already built fibrillar morphology.

Electroless deposition of Ag in slightly acidic solutions

Figure 6 shows open circuit potential (OCP) transients measured after dipping PAMPSA-doped PANI layers with one and the same polymerisation charge in different Ag-containing solutions. The comparison carried out in the 2 mmol l^{-1} Ag-EDTA solution (Fig. 6a) shows that at pH= 4.2, the potential rises quickly and levels out within 200 s whereas at pH=6.6 the potential change is much slower. The different potential behaviour registered in the course of electroless plating may be attributed to the different oxidation state and conductivity of the polymer layers at the two pH values. As shown in Fig. 5, at pH=6.6 and $E<$ −0.2 V the PAMPSA-doped PANI material is almost completely oxidized and low conducting. On the other hand, in the whole potential range of the OCP transient, registered at pH=4.2, the PAMPSA-doped PANI layer is undergoing oxidative transition and the conductance remains high.
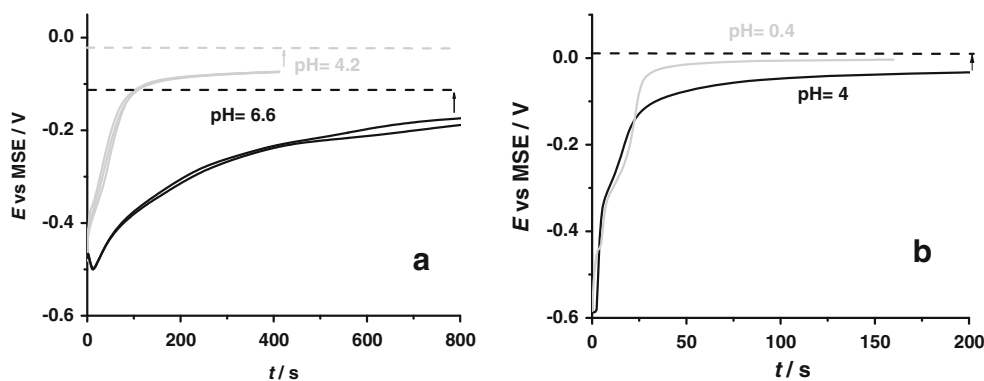
A comparison of the OCP transients registered in two 10 mmol l^{-1} silver-containing solutions, Ag$^+$ ions at pH=0.4 and Ag-EDTA complex anions at pH=4.2, is shown in Fig. 6b. There is no significant influence of the solution composition on the kinetics of the process induced by the change of acidity in the pH range from 0.4 to 4.2 or the complex formation of silver. Thus the strong inhibition of the electroless silver deposition observed at pH=6.6 should be attributed mainly to the loss of conductivity at this pH value and eventually to the stability of the [AgEDTA]$^{3-}$ complex.

Experimental series on electroless silver deposition were carried out in Ag-EDTA solutions with three different concentrations of silver (10.0, 2.0 and 0.4 mmol l^{-1}) and two acidities (pH=4.2 and pH=6.6). In every series, the polymerisation charge of the PAMPSA-doped PANI layers was varied until the amount of deposited silver reached saturation (Fig. 7). Freshly prepared PAMPSA-doped PANI layers were used for each single electroless deposition experiment. The charge q_{Ag}, determined by electrochemical dissolution, was used as a measure for the amount of the deposited metal in each experiment. With few exceptions (open symbols in Fig. 7), the dipping time in these experiments was fixed to 15 s.

Figure 7a shows results for the silver charge obtained at pH=4.2 and the highest concentration of Ag-EDTA species. Prolongation of the dipping time to 300 s (Fig. 7a, open squares) did not result in a higher amount of deposited silver. A linear dependence of q_{Ag} on q_{red} is observed in a wide range of PANI reduction charges with a q_{Ag}/q_{red} ratio of about 50%. A similar charge ratio was already observed for electroless silver deposition in conventional (inorganic anions doped) PANI by using the pH=4.2 silver plating solution [23]. In the latter case, a deviation from linearity started for PANI reduction charges as small as $q_{red}>$ 25 mC cm^{-2}. In contrast, for the PAMSA-doped PANI layers a gradual deviation from the linear relationship is observed at much higher charges ($q_{red}>$80 mC cm^{-2} and $q_{poly}>$400 mC cm^{-2}). This difference should be due to the preserved electroactivity and high conductivity of the

Fig. 6 OCP transients measured at initially reduced PAMPSA-doped PANI layers in different silver plating solutions: **a** 2 mmol l^{-1} Ag-EDTA at pH=4.2 (*grey line*) and pH=6.6 (*black line*) and **b** 10 mmol l^{-1} Ag$^+$, pH=0.4 (*grey line*) and Ag-EDTA, pH=4.2 (*black line*). The *dashed lines* denote the corresponding equilibrium potentials

Fig. 7 Dependence of the silver dissolution charge on the reduction charge of PAMPSA-doped PANI layers for electroless depositions carried out in different Ag-EDTA solutions: **a** 10 mmol l^{-1} at pH=4.2 (*closed* and *open squares*) and pH=6.6 (*closed triangles*); **b** pH=4.2 at different concentrations at 0.4 (*closed* and *open triangles*), 2.0 (*closed* and *open circles*) and 10.0 (*closed squares*) mmol l^{-1} and **c** pH=6.6 at different concentrations as in (**b**). The *closed symbols* are obtained with 15 s dipping time. The *open symbols* are obtained with prolonged dipping times up to 300 s
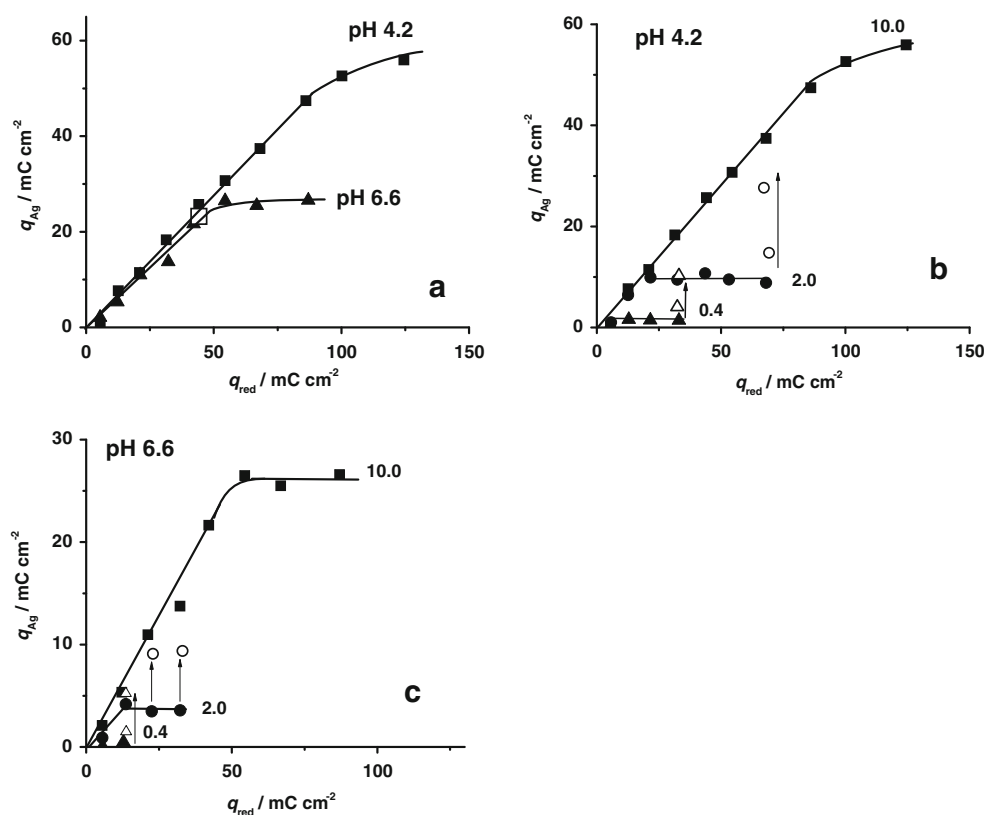
PAMPSA-doped PANI layers in the entire potential range where the electroless deposition occurs.

In the pH=6.6 case (Fig. 7a), the linear dependence of q_{Ag} on q_{red} holds in a narrow range of q_{red} (q_{red}<50 mC cm^{-2} and q_{poly}<250 mC cm^{-2}) with an abrupt loss of linearity observed for higher q_{red} values. In this case, however, the conductivity of the PANI layer in the potential range of the silver electroless deposition (Fig. 5) is much lower. The lower conductivity and the development of the fibrillar structure of the polymer layers impede the charge transfer and the transport of the metal anionic species. These should be the reasons for the observed limitation of the amount of silver deposited in the plating solution at pH=6.6.

At lower concentrations of the silver anion species in the plating solution (Fig. 7b, c) the amount of deposited silver reaches saturation at lower values. By increasing the dipping time in the low concentrated solutions the deposited amount of silver (open symbols in Fig. 7b, c) increases up to the maximal values obtained in the 10 mmol l^{-1} silver-containing solution. In silver plating solutions with low concentration of the metal-containing anions, the process becomes apparently limited by the diffusion of these species in the solution. Thus by a proper choice of concentration of the metal-containing ions and the dipping time it is possible to fix the amount of silver deposited on polymer layers with very different thicknesses.

SEM of the electroless-deposited silver on PAMPSA-doped PANI layers

Figure 8 shows SEM images of Ag-modified PANI layers obtained in 10 mmol l^{-1} Ag-containing solutions with pH= 4.2 (plots a, b, e and f) and pH=6.6 (plots c, d, g and h). The reduction charges of the polymer layers were chosen in a way to have data corresponding to the linear part of the q_{Ag} vs q_{red} relationships (35 mC cm^{-2}) and to the saturation regions (81 and 112 mC cm^{-2}) for the two acid solutions (Fig. 7a). In all cases, the silver particles decorate the most protruding morphology features at the polymer surface with fibrillar structure. Local EDX analysis of the regions where no Ag particles are visibly detected has shown the absence of silver species. Closer inspection of the Ag-decorated spots reveals the formation of densely packed silver grape-like agglomerates (Fig. 8e–h) with diameters of the single particles below 1 μm. The difference between the silver deposit obtained in the two plating solutions is in the size and size distribution of the particles. A larger mean size and a narrower size distribution are characteristic for the Ag

Fig. 8 SEM pictures of PAMPSA-doped PANI layers after Ag-electroless deposition in 10 mmol l^{-1} Ag-EDTA solutions at pH=4.2 (**a**, **b**, **e** and **f**) and pH=6.6 (**c**, **d**, **g** and **h**). Specimens with different reduction charges were used: **a**, **c**, **e**, **g** q_{red}=36 mC cm^{-2}, **b**, **f** q_{red}= 112 mC cm^{-2} and **d**, **h** q_{red}=81 mC cm^{-2}
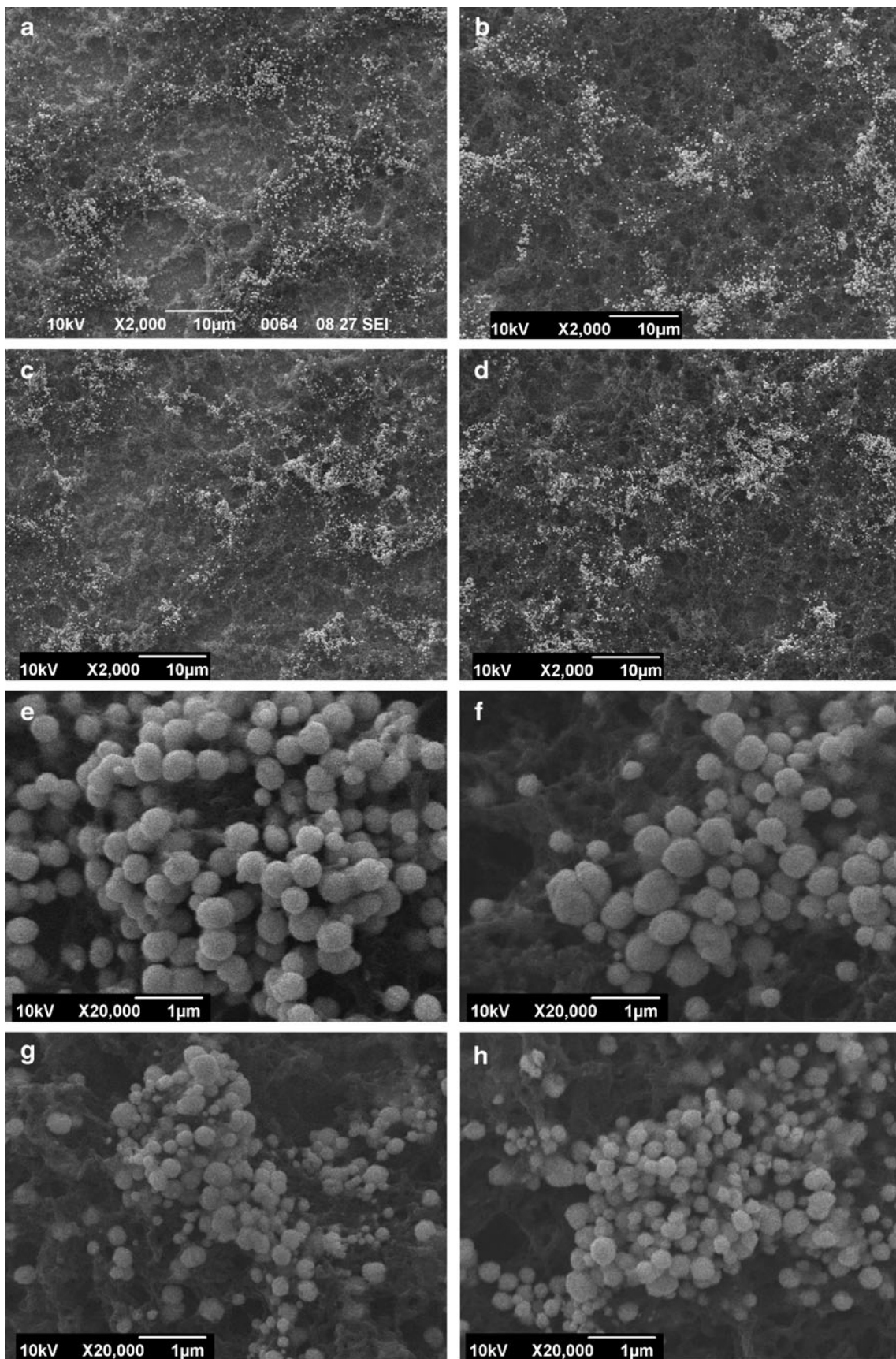
particles deposited in the more acidic solution. This means that in the pH=4.2 plating solution the silver particles nucleate almost instantaneously and grow to a similar size whereas a slower, progressive process of appearance of the silver particles is characteristic for the pH=6.6 plating solution. The different types of the nucleation process (instantaneous and progressive) should relate to the difference in the initial overpotentials in the two plating solutions (Fig. 6a). (The overpotential in both cases is defined as the difference between the actual open circuit potential and the equilibrium potential in the corresponding plating solution). The use of thicker PAMPSA-doped PANI layers (Fig. 8b, d) results in further agglomeration of the Ag particles in the preferred morphological locations.

Similar observation were made for PAMPSA-doped PANI layers (q_{red}=35 mC cm^{-2}) with silver plated in the two 2 mmol l^{-1} Ag-EDTA solutions (Fig. 9). A less dense population of silver species was found on the surface with clearly isolated individual particles with smaller size and rougher surface. A narrower size distribution of the silver particles is observed again in the Ag-EDTA solution with lower pH value.

Conclusions

The present study of the electrochemical characteristics of PAMPSA-doped PANI layers in slightly acidic solutions and on the electroless silver deposition carried out by using the polymer layer as reductant shows several interesting aspects concerning the intrinsic properties of the polymer layers.

The main amount of electroless-deposited silver in our system is detected on the outer polymer surface. A similar result was also obtained in the case of silver electroless deposition on polypyrrole and poly(3,4-ethylenedioxythio-phene) layers [28]. A highly non-homogeneous distribution of the metallic phase over the surface is observed, the most protruding fibrillar polymer structures favouring the electroless silver deposition. The silver particles accumulate at preferred polymer sites with better ability to initiate and sustain the coupled polymer oxidation/metal ions reduction process. These sites should be in contact with well conducting polymer domains playing the role of reservoirs of electrons, necessary to sustain reduction of the silver-containing ions. Thus, the inhomogeneity with respect to the ability of the PAMPSA-doped polymer surface to act as
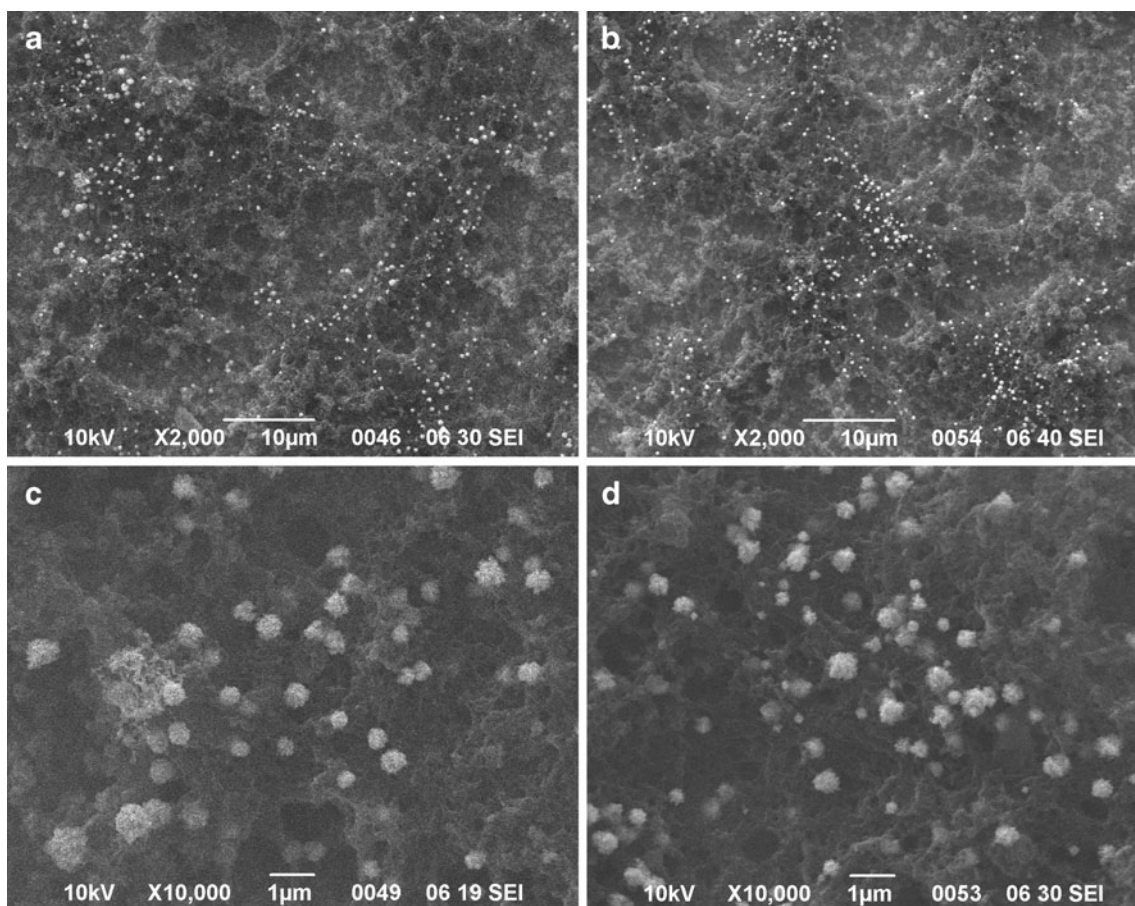
Fig. 9 SEM pictures of PAMPSA-doped PANI layers after Ag-electroless deposition in 2 mmol l^{-1} Ag-EDTA plating solutions at pH=4.2 (**a, c**) and pH=6.6 (**b, d**), q_{red}=37 mC cm^{-2}

a reductant for metal ions should reflect differences in local conductivity. At higher pH value of the metal plating solution the strongly decreased conductivity of the PANI layers impedes the charge transfer within the well conducting polymer domains and lower amounts of metal become deposited on the polymer surface.

The charge transfer within the polymer phase is not the only factor influencing the electroless deposition process. As pointed out in [28] mass transport of the metal-containing ions in the solution and across the polymer layer as well as electron charge transfer for the reduction of the metal-containing ions and finally, metal nucleation phenomena may control the overall process. The formation of relatively big metal particles (with equal sizes) in the high concentrated solutions gives evidence for easy nucleation and growth of the metal phase. At low concentration of the metal-containing anionic species the diffusion in the electrolyte solution becomes the prevailing factor and limits the amount of deposited metal. Nevertheless, the difference in the maximal amount of silver obtained at low concentration and different acidities of the plating solutions shows that either the charge transfer across the polymer phase or the charge transfer involved in the reduction of the two different silver anionic complexes ([AgHEDTA]$^{2-}$ and [AgEDTA]$^{3-}$) still play an important role.

Finally, the use of PAMPSA-doped PANI layers for the electroless deposition of silver provides the possibility to increase markedly the amount of deposited metal in comparison to the use of conventional (inorganic anion doped) PANI layers. This is due to the special role of the immobilised polysulfonic acid providing a material with preserved elctroactivity and conductivity in slightly acidic solutions.

References

1. Inzelt G (2008) Conducting polymers. A new era in electrochemistry. Springer, Berlin
2. Tsakova V (2008) J Solid State Electrochem 12:1421
3. Tsakova V (2010) In: Eftekhari A (ed) Nanostructured conductive polymers. Wiley, Chichester, p 289
4. Pillalamarri SK, Blum FD, Tokuhiro AT, Bertino MF (2005) Chem Mater 17:5941
5. Khanna PK, Singh N, Charan S, Viswanath AK (2005) Mat Chem Phys 92:214
6. Du J, Liu Z, Han B, Li Z, Zhang J, Huang Y (2005) Micropor Mesopor Mater 84:254
7. Huang LM, Tsai CC, Wen TC, Gopalan A (2006) J Polym Sci A 44:3843
8. Huang LM, Wen TC (2007) Mat Sci Engineer A 445–446:7
9. Neelgund G, Hrehorova E, Joyce M, Bliznyuk V (2008) Polym Int 57:1083
10. De Barros RA, De Azevedo WM (2008) Synth Met 158:922
11. Lee Y, Park J, Jun Y, Kim D, Lee J, Kim Y, Oh S (2008) Synth Met 158:143
12. Li X, Gao Y, Liu F, Gong J, Qu L (2009) Mater Lett 63:467
13. Blinova NV, Stejskal J, Trchová M, Sapurina I, Ciric'-Marjanovic G (2009) Polymer 50:50
14. Gniadek M, Bak E, Stojek Z, Donten M (2010) J Solid State Electrochem 14:1303
15. Bober P, Trchova M, Prokes J, Varga M, Stejskal J (2011) Electrochim Acta 56:3580
16. Garai A, Chatterjee S, Nandi AK (2010) Polym Eng Sci 50:446
17. Dimeska R, Murray PS, Ralph SF, Wallace GG (2006) Polymer 47:4520
18. Bouazza S, Alonzo V, Hauchard D (2009) Synth Met 159:1612
19. Stejskal J, Prokes J, Sapurina I (2009) Mater Lett 63:709
20. Stejskal J, Trchová M, Brozová L, Prokes J (2009) Chem Pap 63:77
21. Stejskal J, Trchová M, Kovárová J, Brozová L, Prokes J (2009) React Funct Polym 69:86
22. Zhang AQ, Cui CQ, Lee JY, Loh FC (1995) J Electrochem Soc 142:1097
23. Ivanov S, Tsakova V (2005) Electrochim Acta 50:5616
24. Wang HL, Li W, Jia QX, Akhadov E (2007) Chem Mater 19:520
25. Tsakova V, Milchev A (1991) Electrochim Acta 36:1151
26. Hernandez N, Ortega JM, Choy M, Ortiz R (2001) J Electroanal Chem 515:123
27. Ivanov S, Tsakova V (2004) Electrochim Acta 49:913
28. Ocypa M, Ptasinska M, Michalska A, Maksymiuk K, Hall EAH (2006) J Electroanal Chem 596:157
29. Welch CM, Banks CE, Simm AO, Compton RG (2005) Anal Bioanal Chem 382:12
30. Cui K, Song YH, Yao Y, Huang ZZ, Wang L (2008) Electrochem Commun 10:663
31. Zhao B, Liu Z, Liu Zh, Liu G, Li Zh, Wang J, Dong X (2009) Electrochem Commun 11:1707
32. Quan H, Park SU, Park J (2010) Electrochim Acta 55:2232
33. Lin L, Qiu P, Cao X, Jin L (2008) Electrochim Acta 53:5368
34. Tashkhourian J, Hormozi Nezhad MR, Khodavesi J, Javadi S (2009) J Electroanal Chem 633:85
35. Yang GW, Gao GY, Wang C, Xu CL, Li HL (2008) Carbon 46:747
36. Taheri A, Noroozifar M, Khorasani-Motlagh M (2009) J Electroanal Chem 628:48
37. Qin X, Wang H, Mao Z, Wang X, Fang Y, Chen Q, Shao X (2011) Talanta. doi:10.1016/j.talanta.2011.01.064.
38. Rai M, Yadav A, Gade A (2009) Biotechnol Advances 27:76
39. Lyutov V, Georgiev G, Tsakova V (2009) Thin Solid Films 517:6681
40. Lyutov V, Tsakova V, Bund A (2011) Electrochim Acta 56:4803
41. Hao Q, Kulikov V, Mirsky VM (2003) Sens Act B 94:352
42. Kulikov V, Mirsky VM, Delaney T, Donoval D, Koch AW, Wolfbeis OS (2005) Meas Sci Technol 16:95
43. Lange U, Mirsky VM (2008) J Electroanal Chem 622:246
44. Skoog DA, West DM, Heller FJ, Crouch SR (2004) Fundamentals of Analytical Chemistry. Thomson-Brooks/Cole, New York
45. Yue J, Wang ZH, Cromack KR, Epstein AJ, MacDiarmid AG (1991) J Am Chem Soc 113:2665
46. Xu JJ, Zhou DM, Chen HY (1998) Fresenius J Anal Chem 362:234
47. Milzcarek G (2007) Electrochem Commun 9:123
48. Tarver J, Yoo JE, Dennes TJ, Schwartz J, Loo YL (2009) Chem Mater 21:280